Divalent Calcium Ions Inhibit the Penetration of Protamine through the Polysaccharide Brush of the Outer Membrane of Gram-Negative Bacteria

ARTICLE *in* LANGMUIR · AUGUST 2003

Impact Factor: 4.46 · DOI: 10.1021/la030193e

Divalent Calcium Ions Inhibit the Penetration of Protamine through the Polysaccharide Brush of the Outer Membrane of Gram-Negative Bacteria

D. A. Pink,*,† L. Truelstrup Hansen,‡ T. A. Gill,‡ B. E. Quinn,† M. H. Jericho,§ and T. J. Beveridge||

Department of Physics, St. Francis Xavier University, Antigonish, Nova Scotia, Canada B2G 2W5, Department of Food Science and Technology, Dalhousie University, P.O. Box 1000, Halifax, Nova Scotia, Canada B3J 2X4, Department of Physics, Dalhousie University, P.O. Box 1000, Halifax, Nova Scotia, Canada B3H 3J5, and Department of Microbiology, University of Guelph, Guelph, Ontario, Canada N1G 2W1

Received May 6, 2003. In Final Form: July 18, 2003

Protamine is a cationic antimicrobial peptide, which inhibits or kills a number of Gram-negative bacteria, including *Pseudomonas aeruginosa* and *Escherichia coli*. Electrostatic interactions between the outer leaflet of the membrane and protamine are thought to be important for the antimicrobial effect. We hypothesized that divalent ions would compete with protamine for binding to the charged O-sidechain of the liposaccharide and expel protamine from the O-sidechains. Experimentally it was shown that increasing concentrations of divalent cations (Ca^{2+} and Mg^{2+}) reduced the antimicrobial effect of protamine on *P. aeruginosa* PA01 and *E. coli*. We also modeled the electrostatic interactions between five protamine Y1 molecules from Atlantic herring and the surface of a Gram-negative bacterium possessing charged O-sidechains of the B-band lipopolysaccharides of *P. aeruginosa* PA01 in the presence/absence of calcium ions in an aqueous solution described by linearized Poisson−Boltzmann theory with Debye screening lengths κ^{-1} of 1.0 nm (∼100 mM) and 3.33 nm (∼10 mM). Our conclusions are as follows. [1] A high concentration of calcium ions brought about a slight polysaccharide chain collapse. The calcium ions formed dynamic bridges between the negatively charged O-sidechains on time scales comparable to that of polymer motion. [2] Without the presence of added calcium, all five protamine molecules were trapped in the charged polysaccharide O-sidechain. The probability of finding segments of protamine molecules closer than ∼0.5 nm to the membrane plane (the $x-y$ plane at $z = 0$) was effectively zero. [3] Both the calcium distribution and the protamine distribution, when present separately, were essentially independent of monovalent ionic concentration for both values of κ. [4] When calcium and protamine were present simultaneously, the effects depended strongly upon the monovalent ion concentration. Added calcium effectively prevented protamine from entering the O-sidechain brush. Conclusions 3 and 4 show that the minimum inhibitory concentration should depend on monovalent ion concentration since complex growth media contain multivalent ions. [5] Our experiments confirmed our theoretical prediction that the addition of Ca^{2+} significantly reduced the inhibitory effect of protamine. This also confirmed the importance of electrostatic interactions during the first step in protamine's antibacterial mode of action.

Introduction

A recent consumer-driven trend in food processing is to replace chemical food preservatives, used to improve food safety and quality, with natural antimicrobial alternatives. Similarly, medical researchers are looking for alternatives to commonly used antibiotics due to the development of multidrug-resistant bacterial pathogens, and a great deal of recent work is focused on potential usage of cationic antimicrobial peptides (CAPs).[1] Protamine is a cationic peptide (pI ≈ 10−12) extracted from the sperm cells of vertebrates. Protamine from salmon milt has been used in medicine for years to retard the release of insulin and as an antidote to heparin.[2,3] However, protamine is multifunctional and is antimicrobial toward a range of Gram-positive and Gram-negative bacteria, yeasts, and moulds.[4−9] Protamine is currently being used to preserve starch-based foods in Japan.[10,11] The overall objective of our work is to further investigate the structural−functional properties of protamine for the purpose of exploring alternative uses of this peptide.

Protamine's mode of action at the molecular level is not known, but electrostatic forces are believed to govern the initial interactions between the positively charged protamine and the negatively charged bacterial cell envelope. If the protamine concentration is sufficiently high, this initial binding may subsequently lead to the destruction of the normal cell envelope and cytoplasmic membrane functions and result in growth inhibition or cell death due to loss of the proton motive force (PMF) and leakage of K^+,

† Department of Physics, St. Francis Xavier University.
‡ Department of Food Science and Technology, Dalhousie University.
§ Department of Physics, Dalhousie University.
|| Department of Microbiology, University of Guelph.

(1) Hancock, R. E. W.; Chapple, D. S. *Antimicrob. Agents Chemother.* **1999**, *43* (6), 1317.
(2) Jaques, L. B. *Can. Med. Assoc. J.* **1973**, *108*, 1291.
(3) Brange, J. *Galenics of Insulin*; Springer-Verlag: Berlin, 1987; Chapter 3.
(4) Brock, T. D. *Can. J. Microbiol.* **1958**, *4* (2), 65.
(5) Islam, N. M.; Itakura, T.; Motohiro, T. *Bull. Jpn. Soc. Sci. Fish.* **1984**, *50* (10), 1705.
(6) Kamal, M.; Motohiro, T. *Nippon Suisan Gakkaishi* **1986**, *52*, 1843.
(7) Uyttendaele, M.; Debevere, J. *Food Microbiol.* **1994**, *11*, 417.
(8) Johansen, C.; Gill, T.; Gram, L. *J. Appl. Bacteriol.* **1995**, *78*, 297.
(9) Truelstrup Hansen, L.; Austin, J. W.; Gill, T. A. *Int. J. Food Microbiol.* **2001**, *66*, 149.
(10) Ueno, R.; Fujita, Y.; Yamamoto, M.; Kozakai, H. European Patent Application 0273 606, 1987.
(11) Ueno, R.; Fujita, Y.; Nagamura, Y.; Kamino, Y.; Tabata, A. European Patent Application 0372 091, 1989.

10.1021/la030193e CCC: $25.00
Published on Web 08/29/2003

ATP, and intracellular enzymes.[12−14] Numerous factors will influence bacterial sensitivity to protamine, including cell wall and membrane composition, fluidity, and permeability; proteolytic enzymes; compounds competing for the same binding sites; or the presence of compounds capable of removing available protamine through nonspecific binding. Interfering ions and compounds found in body fluids, biofilms, and food matrixes may necessitate the development of innovative delivery methods so protamine and other CAPs can reach their targets. Such delivery methods will ultimately determine the scope of CAP usage in medicine and food preservation.

Pseudomonas aeruginosa is a well-characterized Gram-negative bacterium which is involved in respiratory tract infections and formation of biofilms. *P. aeruginosa* is often associated with chronic infections in cystic fibrosis patients.[15] Gram-negative bacteria including *Pseudomonas* spp. and *Escherichia coli* are characterized by the presence of an outer membrane containing lipopolysaccharides (LPSs). LPSs present the first barrier which protamine has to penetrate to reach the cytoplasmic membrane and consists of three separate chemical moieties: (1) lipid A possesses acyl chains which insert the LPS molecule into the hydrophobic domain of the membrane bilayer; (2) the core oligosaccharide sits immediately above the lipid A and possesses substituents, such as ketodeoxyoctonate and phosphate (often attached to heptose), with ionizable groups which give this region an overall electronegative charge at neutral pH; and (3) the O-sidechain is attached to the core oligosaccharide, consists of linear chains of sugar residues, and extends (often) tens of nanometers above the outer face of the bilayer. The O-sidechains can be either charged or uncharged, but overall, the core and the O-sidechain form a hydrophilic moiety which extends into the aqueous milieu surrounding the bacterium.

Pseudomonal LPS possesses a lipid A moiety consisting of a β-1,6-linked disaccharide of *N*-hydroxymyristoyl-D-glucosamine which is O-acetylated by β-hydroxymyristic acid with relatively short (C_8−C_{14}) acyl chains extending from this backbone structure.[16] Phosphoryl or pyrophosphoryl groups are located at the reducing terminus of the disaccharide which is additionally phosphorylated at the 4′ position. The core oligosaccharide and the O-sidechain polysaccharides are attached to lipid A and extend outward from the bacterium. Surprisingly, the PA01 strain possesses two separate varieties of LPS on its surface during planktonic growth: A-band LPS (A^+) and B-band LPS (B^+).[17] A^+ is designated as the "common antigen" since it is found on all *P. aeruginosa* strains. It is the chemically simplest of the two LPSs since its terminal O-sidechain consists of a short repeating pattern of an α-D-rhamnose trimer (linked 1→2, 1→3, and 1→3) about 10−20 units long. The O-sidechain of B^+ LPS is more complex and is designated as "serotype LPS" since it possesses the distinctive O-antigen of each strain. The PA01 strain of *P. aeruginosa* is serotype 05, is a common laboratory strain, and has an O-sidechain consisting of a trisaccharide repeating unit of 2-acetamido-3-acetamidino-2,3-dideoxy-D-mannuronic acid (Man[2NAc3N]A), 2,3-diacetamido-D-mannuronic acid (2,3-diNAcManA), and 2-acetamido-2,6-dideoxy-D-galactose (*N*-acetylfucosamine, Fuc2NAc). Serotype 05 can express more than 30 of these repeating trisaccharides on each O-sidechain polymer which sits above a core oligosaccharide of D-glucose, L-α-D-heptose, and 3-keto-3-deoxy-D-mannooctonic acid (ketodeoxyoctonic acid, KDO).

The LPS layer contains Mg^{2+} and/or Ca^{2+} in the KDO-core region. The integrity of this layer was previously demonstrated to be important since the presence of the divalent ion chelating and LPS-disrupting ethylenediaminetetraacetic acid (EDTA) significantly increased the sensitivity of Gram-negative bacteria to protamine.[9]

The purpose of this study was to mathematically model the effects of the electrostatic interactions between the electrically charged O-sidechain polysaccharides of the B-band lipopolysaccharides from *P. aeruginosa* PA01 and protamine molecules in the presence or absence of Ca^{2+}. It was hypothesized that the presence of Ca^{2+} would repel protamine electrostatically such that penetration of protamine into the polyelectrolytic brush would be limited. Experiments were also pursued on the chosen model target microorganisms, *P. aeruginosa* PA01 and *E. coli*, to determine if the theoretical findings agreed with experimental observations.

Experimental Section

Effect of Divalent Ions on the Antimicrobial Properties of Protamine. The antimicrobial efficacy of protamine on B-band *P. aeruginosa* PA01 and three *E. coli* strains [Ec1 (EC961019, serotype O157:H7, Health Canada), Ec17 (EC970112, O157:H7, Health Canada), and Ec22 (ATCC 25922, O6)] in the presence of divalent ions Ca^{2+} and Mg^{2+} was determined experimentally. Protamine minimum inhibitory concentrations (MICs) were determined using the broth dilution assay with the growth indicator Alamar Blue in 96-well microplates as previously described.[9] Briefly, protamine (Clupeine sulfate P4505; Sigma, Oakville, ON, Canada) was dissolved in tryptic soy broth (TSB; Oxoid, Nepean, ON, Canada) (pH 7.0; according to the manufacturer, the endogenous content of monovalent cations is 87 mM Na^+ and 33 mM K^+ and that of divalent cations is 0.6 mM Ca^{2+} and 0.3 Mg^{2+}) and diluted 2-fold to produce final assay concentrations of 5000, 2500, 1250, 625, 313, 156, 78, 39, 20, 10, 5, and 0 μg mL^{-1} (control sample). The test strains were grown overnight in TSB at 30 °C, diluted in TSB, and inoculated in concentrations of 100−1000 cfu per well (50 μL per well). Finally, Alamar Blue (aqueous solution; Medicorp, Montréal, Québec, Canada) was added (5 μL per well). The indicator was not toxic to the bacteria since growth in TSB controls with the indicator was not inhibited. MICs were read after incubation for 24 h at 30 °C as the lowest protamine concentration inhibiting visible color change from blue to pink. The antimicrobial effect of protamine in the presence of Ca^{2+} ($CaCl_2$) or Mg^{2+} ($MgCl_2$) concentrations above those normally found in TSB was tested using a factorial design and reported as protamine MICs at the individual divalent ion concentrations. Protamine (0−5000 μg mL^{-1}) was tested in combination with Ca^{2+} and Mg^{2+} concentrations of 0, 10, 50, 100, and 200 mM. Ca^{2+} and Mg^{2+} were added to the wells as 20 μL (Ca^{2+}) or 40 μL (Mg^{2+}) of concentrated sterile aqueous salt solutions. MIC assays were subsequently conducted as described above with appropriate adjustments to account for the extra aqueous volume. All assays were carried out in duplicate, and where results disagreed, a second experiment was conducted. This was necessary in only 2.5% of experiments, and disagreement was never observed by more than one dilution factor. Values reported are from agreeing replicates.

Modeling and Computer Simulation

LPS O-Sidechains. The density of the O-sidechains is characteristic of an end-grafted polyelectrolyte brush.[18]

(12) Islam, N. M. D.; Oda, H.; Motohiro, T. *Nippon Suisan Gakkaishi* **1987**, *53*, 297.
(13) Johansen, C.; Verheul, A.; Gram, L.; Gill, T.; Abee, T. *Appl. Environ. Microbiol.* **1997**, *63*, 1155.
(14) Stumpe, S.; Bakker, E. P. *Arch. Microbiol.* **1997**, *167*, 126.
(15) Høiby, N. *Int. J. Antimicrob. Agents* **1992**, *1*, 229.
(16) Wilkinson, S. G.; Galbraith, L.; Lightfoot, G. A. *Eur. J. Biochem.* **1973**, *33*, 158.
(17) Riviera, M.; Byran, L. E.; Hancock, R. E. W.; McGroarty, E. J. *J. Bacteriol.* **1988**, *170*, 512.
(18) Lai, P.-Y.; Binder, K. *J. Chem. Phys.* **1992**, *97*, 586.

Our intention was to examine the effects of the interactions between O-sidechains and protamine molecules in the absence and presence of Ca^{2+} ions. While van der Waals interactions are ubiquitous, the dominant interaction that distinguishes between different sugar groups is the electrostatic interaction. Since this is a study of electrostatic effects, we have excluded the possibility of hydrogen bonding, although this model can accommodate that. The presence of the O-sidechain polymer brush renders Derjaguin−Landau−Verwey−Overbeek (DLVO) theory[19] inadequate. A model which takes these observations into account might be difficult to study analytically and must be amenable to computer simulation.

The simulation volume must be large enough to accommodate both the physical size of the O-sidechains and protamine molecules and the range of the interactions. We must be able to simulate up to $\sim 10^2$ O-sidechains, which represents a bacterial surface area of ~ 200 nm^2, together with up to ~ 50 protamine molecules and $\sim 10^3$ divalent cations. Each O-sidechain should be composed of up to ~ 10 trisaccharide groups. In addition, the simulation must sample configurational changes that could occur on time scales of $> 10^{-3}$ s. In this paper, computer simulations involved a low concentration of protamine[5] and ~ 150 Ca^{2+} ions. Because of these demands of a large scale, we did not use atomic models together with a molecular dynamics simulation but instead created a "minimal model" which nonetheless takes into account all of the desired physics so that we can perform sufficiently large-scale computer simulations.

Two questions must be addressed: (a) how are the properties of the solvent represented and (b) how are interfaces and the properties of different materials in contact with the solvent modeled?

(a) Recent work represented the aqueous solution by a dielectric continuum using Poisson−Boltzmann (PB) theory or an extension of it.[20,21] It has been found that PB theories, even linearized PB theories in some cases, are adequate to describe the bulk of an aqueous solution together with monovalent ions. Because of the importance of spatial correlations involving multivalent ions and polyions, however, these must be represented by discrete, localized structures. Our model adopts this approach. The question as to how counterions are treated is important. Very long polyions which possess persistence lengths much greater than their lateral dimensions, such as DNA, have been modeled as totally charge neutral with the system explicitly including the counterions (ref 20 and references therein). Such a system sets up a logarithmic electric potential that results in Manning−Oosawa condensation.[22] In the case of a living bacterium, the question of how total charge neutrality is achieved (bacterium plus surroundings) is open. Our measurements of electrophoretic mobility of *E. coli* (Ec22) indicated an overall negative charge at pH 7 with a zeta potential of −15 mV. It is likely that *P. aeruginosa* also would exhibit an overall negative charge. Accordingly, the condition of total charge neutrality at the cell wall−aqueous solution interface in the neighborhood of the charged O-sidechains should not be imposed.

(b) A more difficult problem is to adequately represent the regions in contact with the aqueous solution where the potentials must satisfy interface boundary conditions.

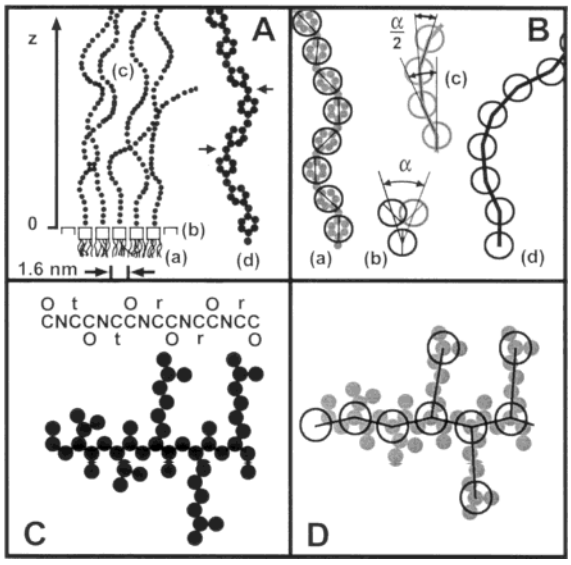

Figure 1. (A) A cross section through the lipopolysaccharides in the outer leaflet of the outer membrane showing the hydrocarbon chains (a), the KDO-core region (b), and the polysaccharide O-sidechains (c). The origin of the *z*-axis is shown. Also shown is a polysaccharide O-sidechain with rotations around two oxygens indicated by arrows (d). (B) The model used showing the mapping of the sugar groups onto "sugar spheres" (a), the angle α (b,c), and a model O-sidechain with many rotations (d). (C) A portion of the protamine sequence with the corresponding atomic representation. (D) A model protamine molecule in which the atomic moieties (gray) are replaced by spheres connected by bonds (black).

This has been addressed by Netz and others,[23] and we shall refer to it again below. Recent work on modeling a polyelectrolyte brush was carried out by Zhulina et al.[24] for long, weakly charged polymer chains. The charges on the polymers, however, were all of the same sign, unlike our case of a bacterial interface, where the polymers contain both positively and negatively charged residues. Zhulina et al.[24] developed a self-consistent-field theory of a brush of intrinsically flexible polymer chains, assumed to obey Gaussian statistics on length scales much shorter than the polymer lengths. However, they did not consider the dielectric properties of the surface to which the polymers were grafted. The O-sidechains modeled here are semiflexible and are not assumed to obey Gaussian statistics.

We represented each LPS O-sidechain as a linear polymer tethered to the surface of a disk, of radius r_{disk}, representing the cross-sectional area of the oligosaccharide KDO-core and lipid A. In our case, $r_{disk} = 0.8$ nm. The set of disks represented the $x-y$ plane (with $z = 0$) of the outer membrane interface with the environment. The disk could move laterally in this plane, but not out of it, to represent LPS lateral diffusion in the plane of the membrane. We used periodic boundary conditions. Each sugar of an O-sidechain was represented by a sphere of radius r_{sug} with either one charge (charged sugars from B-band LPS) or no charge (uncharged sugars from A-band LPS) located at the center of each sphere. The centers of nearest neighbor spheres were connected by bonds of length L_0.

Figure 1A shows a typical lipopolysaccharide molecule with its lipid A segment (a), the KDO-core segment (b), and the polysaccharide O-sidechain (c) with the sugar

(19) Hermansson, M. *Colloids Surf., B* **1999**, *14*, 105.
(20) For example: Deserno, M.; Holm, C.; May, S. *Macromolecules* **2000**, *33*, 199.
(21) Vlachy, V. *Annu. Rev. Phys. Chem.* **1999**, *50*, 145.
(22) Manning, G. S. *Q. Rev. Biophys.* **1978**, *11*, 179.
(23) Netz, R. R. *Phys. Rev. E* **1999**, *60*, 3174.
(24) Zhulina, E. B.; Wolterink, J. K.; Borisov, O. V. *Macromolecules* **2000**, *33*, 4945.

groups connected by oxygen atoms. Twisting of the chain arises only through rotations around the oxygen atoms as shown (d), where two rotations around oxygen atoms are indicated by arrows. Figure 1B shows our representations of these sugar chains. A sugar group sphere possesses an axis as shown. The angle α is the internal angle between lines connecting the centers of adjacent sugar groups when a rotation of 180° around the oxygen is carried out. Comparing panels b and c of Figure 1B, one sees that the forward angle between successive bonds is $\alpha/2$. Figure 1B(d) shows a chain conformation with many twists. This off-lattice model is similar to minimal models considered by others.[18,25,26] When moving the polymers, we used the bond-stretching technique:[25,27] bonds could change their lengths by $\pm\Delta L$. Similarly, the angle, $\alpha/2$, between successive bonds was permitted a variation of $\pm\Delta\alpha$. Figure 1C shows a portion of the sequence of protamine Y1 from Atlantic herring (NCBI website, http://www.ncbi.nlm.nih.gov/) together with a pictorial representation of it. Figure 1D shows our model (black) of that segment (gray). The polypeptide chain of a protamine molecule was represented as a linear polymer composed of spheres, of radius r_{pep}, representing the peptide groups (HN−CR−CO) connected by stretchable bonds. Protamine Y1 contains 20 arginine residues, and each such residue was represented by a positively charged sphere, of radius r_{guan}, attached, by a bond, to the appropriate peptide group. Hydrated divalent cations (Ca^{2+}) were represented by spheres of radius r_I with a double proton charge at the center.

Electrostatic Interactions. The aqueous solution and the hydrophobic lipid A region of the LPS complex were represented by two continua of dielectrics with relative permittivities 81 and 5, respectively, with the two regions separated by a plane at $z = 0$.[28,29] The half-spaces $z > 0$ and $z < 0$ were occupied by the aqueous solution and a dielectric representing the hydrophobic region, respectively. We made no attempt to take into account a z-dependent permittivity in the neighborhood of the interface. We used the results of linearized Poisson−Boltzmann theory to obtain the electric potential at a point $\vec{R} = x\vec{x} + y\vec{y} + z\vec{z}$, outside the hydrophobic region, due to an electric charge, Q, located at $\vec{R}_0 = x_0\vec{x} + y_0\vec{y} + z_0\vec{z}$ also in the aqueous solution. Here $\vec{x}$, $\vec{y}$, and $\vec{z}$ are unit vectors with $\vec{z}$ perpendicular to the plane of the membrane−water interface.

In the presence of an interface separating the two spaces, this calculation is not trivial. This has been addressed by Netz,[23] who derived expressions for the electrical potential at $\vec{R}$ (ref 23, eqs 14 and 15). In the case where the relative permittivity of the hydrophobic lipid A region, $\epsilon_{hp} = 5$, is very much less than that of the aqueous solution, $\epsilon_w = 81$, the expression for the potential simplifies (ref 23, eq 20). This is given for that case by eq 20.[23] In our expression for the potential, we have included the image charge factor, $\chi = (1 - \eta)/(1 + \eta)$ with $\eta = \epsilon_{hp}/\epsilon_0 \approx 0.06$. The electrical potential at $\vec{R}$ becomes

$$V(Q,\vec{R}_0,\vec{R}) = (1/4\pi\epsilon_w\epsilon_0)\sum_j Q_j f(|\vec{R}_j|) \qquad (1)$$

where the sum is over $j = 1$ to 2 and

$$f(|\vec{R}_j|) = \frac{e^{-\kappa|\vec{R}_j|}}{\vec{R}_j} \qquad (2)$$

$$\vec{R}_1 = \vec{R} - \vec{R}_0$$

$$\vec{R}_2 = \vec{R} - \vec{R}_0 + 2z_0\vec{z}$$

$$Q_1 = Q$$

$$Q_2 = \chi Q$$

$$\chi = (1 - \eta)/(1 + \eta)$$

Here ϵ_0 is the permittivity of free space and κ^{-1} is the Debye screening length. The potential (eq 1) goes to the two correct limiting values as $\epsilon_{hp} \to 0$ or as $\kappa \to 0$. In the usual mean field model of an aqueous solution at temperature T, with a single species of symmetrical electrolyte possessing valence ζ, κ is related to the bulk concentration of ions[28] by

$$\kappa^2 = \frac{2e^2 n_0 \zeta^2 \beta}{\epsilon_0 \epsilon_w} \qquad (3)$$

where e is the magnitude of the electronic charge, n_0 is the bulk concentration of ions in the solution, and $\beta = 1/k_B T$ with k_B = Boltzmann's constant. From this, one sees that κ is proportional to $I^{1/2}$, where I is the ionic strength. Thus, at room temperature a value of $\kappa = 1$ nm^{-1} corresponds to $I \approx 10^{-1}$ M and $\kappa = 0.3$ nm^{-1} corresponds to $I \approx 10^{-2}$ M. The first value is typical of an aqueous solution at a physiological ionic concentration.

Computer Simulation. We made use of the Monte Carlo (MC) simulation procedure using the Metropolis algorithm which ensures that the system will come to thermal equilibrium.[18,30] At each Monte Carlo step, we attempted to change the position of each Ca^{2+} ion. Because of the sizes of the polysaccharide sugar groups, the protamine peptide groups, and the protamine arginine groups relative to that of a Ca^{2+} ion, we allowed the last named to move 10 times more often, on the average, than did the sugar groups and the peptide or arginine spheres. This was implemented at each Monte Carlo step, by attempting to change the position of each O-sidechain or protamine sphere, with a probability of 0.1, by randomly choosing a new position according to the limitations on bond length and angle described above. Each disk, to which the O-sidechains were attached, was moved laterally in the x−y plane. If the energy of the system before the attempted change was E_i and it is E_f after the change, then we defined $\Delta E = E_f - E_i$. If $\Delta E \le 0$, the change was implemented, but if $\Delta E > 0$, then a random number, $0 \le r < 1$, was chosen so that if $r \le \exp(-\beta\Delta E)$ then the change was implemented. Otherwise, the system remained in the state before the change was attempted. The temperature chosen was $T = 303$ K. The system was equilibrated for 10^6 Monte Carlo steps, and the properties of the system were measured for a further 10^4 to $> 10^6$ steps. Our systems contained 64 polymer chains each composed of five (charged) trisaccharide units and each tethered to the center of a disk. Periodic boundary conditions were used. The values used were $r_{sug} = 0.15$ nm and $L_0 = 0.52$ nm, and the Carmesin−Kremer bond-stretching technique was employed.[26] The structure and flexibility of the chains were accounted for by restricting any two successive bonds

(25) Chakrabarti, A.; Nelson, P.; Toral, R. *J. Chem. Phys.* **1994**, *100*, 748.
(26) Stevens, M. J.; Kremer, K. *Phys. Rev. Lett.* **1993**, *71*, 2228.
(27) Carmesin, I.; Kremer, K. *Macromolecules* **1988**, *21*, 2819.
(28) For example: Israelachvili, J. N. *Intermolecular and Surface Forces*; Academic Press: London, 1985.
(29) Pink, D. A.; Belaya, M.; Levadny, V.; Quinn, B. *Langmuir* **1997**, *13*, 1701.
(30) *Applications of the Monte Carlo Method in Statistical Physics*; Binder, K., Ed.; Springer-Verlag: Heidelberg, Germany, 1984.

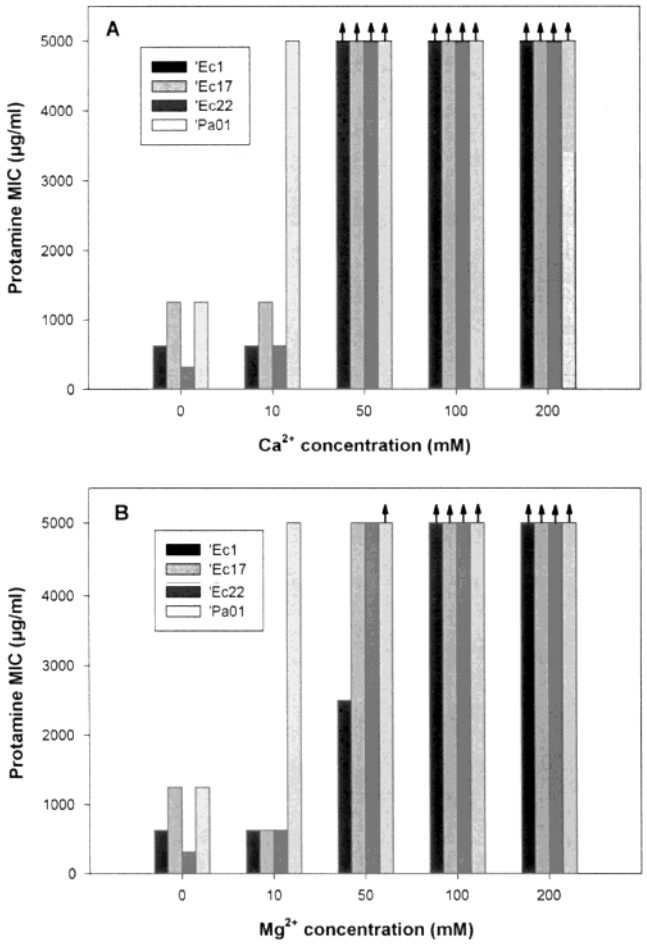

Figure 2. Inhibitory effect of protamine in combination with divalent ions on three *E. coli* (Ec) strains and *P. aeruginosa* PA01 (Pa) at 30 °C: (A) calcium and (B) magnesium. [↑] indicates that growth was not inhibited by the highest protamine concentration (5000 μg/mL) in the assay.

to relative angles of $30 \pm 5°$ so that $\alpha = 60 \pm 10°$. Charges ($\pm 1.6 \times 10^{-19}$ C) were located at the centers of each sugar sphere as appropriate. The value of r_{pep}, the radius of the peptide group sphere, was 0.18 nm, while the radius of a guanidine group sphere, r_{guan}, was taken as 0.15 nm. Hydrated divalent cations were represented by doubly charged spheres of radius $r_I = 0.18$ nm.

Results and Discussion

Antimicrobial Efficacy of Protamine in the Presence of Divalent Cations Ca^{2+} and Mg^{2+}. Experiments were carried out to test whether the predictions obtained by the computer simulations of the electrostatic interactions between lipopolysaccharide O-sidechains, calcium, and protamine could be confirmed. The experimental testing was carried out in TSB broth with a calculated ionic strength, *I*, of ~130 mM. *P. aeruginosa* PA01 and the three *E. coli* strains were inhibited by protamine alone with MICs ranging from 313 to 1250 μg mL^{-1} (Figure 2). The addition of increasing concentrations of divalent Ca^{2+} and Mg^{2+} ions markedly decreased the antibacterial effect of protamine on the bacteria. Islam et al.[31] similarly reported that addition of divalent cations decreased the effect of protamine on the Gram-positive *Bacillus subtilis*.

Addition of only 10 mM Ca^{2+} or Mg^{2+} ($I \sim 160$ mM) increased the protamine MICs for *P. aeruginosa* PA01 from 1250 (control) to 5000 μg mL^{-1} (Figure 2). At divalent ion concentrations at or above 50 mM ($I \sim 280$ mM), there was no longer any inhibitory effect of protamine on *P. aeruginosa* PA01.

The *E. coli* strains remained sensitive to protamine as the divalent cation concentration was increased by 10 mM resulting in MICs ranging between 625 and 1250 μg mL^{-1} and 625 μg mL^{-1} for Ca^{2+} or Mg^{2+}, respectively (Figure 2). The presence of 10 mM Mg^{2+} lowered the protamine MIC for one strain (Ec17). Obviously, *E. coli* is a relatively sensitive Gram-negative bacterium with a previously reported protamine MIC of 625 μg mL^{-1}.[9] Interestingly, protamine inhibited all *E. coli* strains in the presence of 50 mM Mg^{2+} while at the same concentration of Ca^{2+} none of the strains were inhibited by the maximum protamine concentration of 5000 μg mL^{-1}. This would indicate that Ca^{2+} more effectively kept protamine out of the polyelectrolyte brush than did Mg^{2+}. A hydrated Ca^{2+} ion is larger than a hydrated Mg^{2+} ion, with a Ca−O distance to the first hydration shell of about 0.23 nm[32] compared to the corresponding Mg−O distance of about 0.2 nm.[32] It is thus possible that hydrated Ca^{2+} ions form larger and more effective (dynamical) bridges between the LPS charged polysaccharide polymers than do Mg^{2+} ions. Also, the polarizability of calcium (0.0228 nm^3)[33] is twice as large as that of magnesium (0.0106 nm^3),[34] and this might have consequences for forming dynamical cationic bridges.

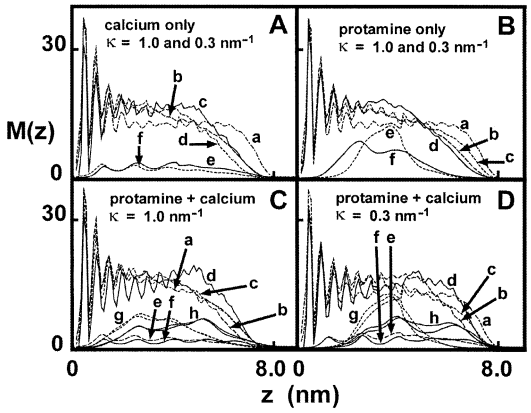

Figure 3. Mass distributions, $M_{OS}(z)$, $M_P(z)$, and $M_{Ca}(z)$, of O-sidechains, protamines, and Ca^{2+}, as functions of distance away from the KDO-core plane ($z = 0$). (A) No protamine. Without Ca^{2+}: $M_{OS}(z)$ for $\kappa = 0.3$ nm^{-1} (a) and $\kappa = 1.0$ nm^{-1} (b). With Ca^{2+}: $M_{OS}(z)$ for $\kappa = 0.3$ nm^{-1} (c) and $\kappa = 1.0$ nm^{-1} (d); $M_{Ca}(z)$ for $\kappa = 0.3$ nm^{-1} (e) and $\kappa = 1.0$ nm^{-1} (f). (B) No calcium. Without protamine: $M_{OS}(z)$ for $\kappa = 0.3$ nm^{-1} (a) and $\kappa = 1.0$ nm^{-1} (b). With protamine: $M_{OS}(z)$ for $\kappa = 0.3$ nm^{-1} (c) and $\kappa = 1.0$ nm^{-1} (d); $M_P(z)$ for $\kappa = 0.3$ nm^{-1} (e) and $\kappa = 1.0$ nm^{-1} (f). (C) $\kappa = 1.0$ nm^{-1}. No Ca^{2+}, no protamine: $M_{OS}(z)$ (a). With Ca^{2+}, no protamine: $M_{OS}(z)$ (b) and $M_{Ca}(z)$ (e). No Ca^{2+}, with protamine: $M_{OS}(z)$ (c) and $M_P(z)$ (g). With Ca^{2+}, with protamine: $M_{OS}(z)$ (d), $M_{Ca}(z)$ (f), and $M_P(z)$ (h). (D) $\kappa = 0.3$ nm^{-1}. No Ca^{2+}, no protamine: $M_{OS}(z)$ (a). With Ca^{2+}, no protamine: $M_{OS}(z)$ (b) and $M_{Ca}(z)$ (e). No Ca^{2+}, with protamine: $M_{OS}(z)$ (c) and $M_P(z)$ (g). With Ca^{2+}, with protamine: $M_{OS}(z)$ (d), $M_{Ca}(z)$ (f), and $M_P(z)$ (h). Note that there are two distributions shown for each protamine case, curves g and h. This shows that once it has come to equilibrium, the protamine distribution undergoes small oscillations along the *z*-axis with an amplitude of ~0.5 nm with a period of $\sim 10^6$ MC steps. The two distributions are 10^6 MC steps apart.

Computer Simulations. Figure 3 shows typical equilibrium results for the mass distribution of charged

(31) Islam, N. M. D.; Motohiro, T.; Itakura, T. *Bull. Jpn. Soc. Sci. Fish.* **1985**, *51*, 811.

(32) Pavlov, M.; Siegbahn, P. E. M.; Sandström, M. *J. Phys. Chem. A* **1998**, *102*, 219.

(33) http://www.scescape.net/~woods/elements/calcium.html.

(34) http://www-tech.mit.edu/Chemicool/elements/magnesium.html.

O-sidechains, $M_{OS}(z)$, of protamine, $M_P(z)$, and of calcium ions, $M_{Ca}(z)$, as functions of distance, z, from the membrane for two values of the Debye screening length, $\kappa^{-1} = 1$ nm and $\kappa^{-1} = 3.3$ nm. Figure 3A shows the effects of adding calcium ions to the polymer brush. The calcium ions were added in a region outside the brush so that they interacted only weakly. The persistence length of the O-sidechain is ~5 nm, and this gave rise to chain ordering close to the membrane plane as shown by the oscillations at low z. The greater electrostatic charge repulsion when $\kappa = 0.3$ nm^{-1}, compared to when $\kappa = 1.0$ nm^{-1}, caused the charged polysaccharide chains to extend further along z by about 10% more in the former case (a) than in the latter (b). This effect was reversed when calcium was added: the longer-ranged electrostatic interaction caused the calcium ions to bring about greater chain collapse for $\kappa = 0.3$ nm^{-1} (c) than for $\kappa = 1.0$ nm^{-1} (d). We can also see that the calcium distributions inside the brush (e,f) show spatial correlation with the negatively charged sugar spheres. More calcium ions were pulled into the brush for $\kappa = 0.3$ nm^{-1} (e) than for $\kappa = 1.0$ nm^{-1} (f). Figure 3B shows the effects of adding five protamine molecules alone. The molecules were inserted at a distance outside the polymer brush so that they interacted only weakly with it. Eventually, all molecules became trapped inside the brush. The effect of the polypeptide was to cause greater chain collapse for $\kappa = 1.0$ nm^{-1} (d) than for $\kappa = 0.3$ nm^{-1} (c), opposite to the effect of calcium. Indeed, the chain distributions with protamine trapped inside show a similarity to those of the chains without either protamine or calcium. It is not surprising then that the protamine distributions are nearly identical for both $\kappa = 0.3$ nm^{-1} (e) and $\kappa = 1.0$ nm^{-1} (f). Note also that protamine does not reach the plane $z = 0$: the probability of finding any protamine moieties at $z < 0.5$ nm is essentially zero. The distributions are broad, extending from $z \approx 0.5$ nm to $z \approx 9$ nm with maxima at $z \approx 2.7$ nm ($\kappa = 1.0$ nm^{-1}) and $z \approx 2.2$ and 3.5 nm ($\kappa = 0.3$ nm^{-1}).

Figure 3C shows the effect of adding both calcium and protamine when $\kappa = 1.0$ nm^{-1} (h). We see that although there are small changes in the O-sidechain distribution as calcium and protamine are added, the effect of calcium is to broaden the protamine distribution from $z \approx 0.8$ nm to $z \approx 9.3$ nm. For $z < 4.7$ nm, the probability of finding a protamine moiety has been reduced by ~30% when calcium is added compared to when it is absent. If this shift in the predicted distribution of protamine is related to its antimicrobial efficacy, then we must predict that the effect of calcium will be to increase the MIC. This "protamine expelling" effect is increased when $\kappa = 0.3$ nm^{-1} (h). Two equilibrium distributions with/without calcium are shown in order to illustrate the small oscillations that take place along the z axis. In this case, the calcium has driven the protamine to the top of the O-sidechain brush. When calcium is present, the probability of finding a protamine moiety for $z < 3$ nm is very small compared to the case in which calcium is absent, when the protamine distributions exhibit maxima lying between 2.5 and 4 nm. The maximum for the case of calcium present lies at $z \approx 6$ nm.

Further, the relative effect upon the MIC of adding calcium will be more pronounced for $\kappa = 0.3$ nm^{-1} ($I \approx 10$ mM) than for $\kappa = 1.0$ nm^{-1} ($I \approx 100$ mM). If the salt concentration is reduced in the model system so that the electrostatic interaction becomes longer-ranged, then the MIC of protamine will become relatively more susceptible to electrostatic effects due to the presence of calcium. However, this was not analyzed experimentally.

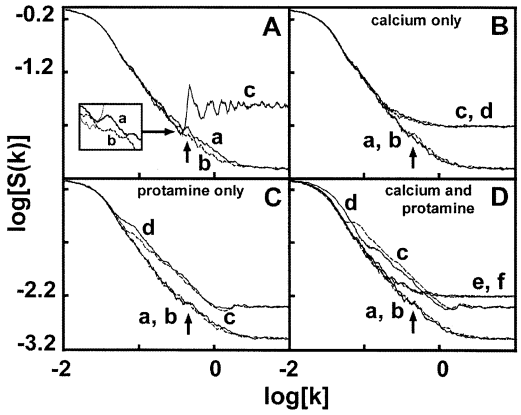

Figure 4. Static structure functions, log[$S(k)$] vs log[k]. The units of k are Å^{-1}. The static structure functions $S_{OS}(k)$, $S_P(k)$, and $S_{Ca}(k)$ were obtained by averaging over k-vectors lying in the xy-plane. $S_{OS}(k)$ is determined by the positions of the centers of all O-sidechain sugar spheres, $S_P(k)$ by the centers of all protamine spheres, and $S_{Ca}(k)$ by the centers of all calcium spheres. In all cases, $S_{OS}(k)$ for $\kappa = 0.3$ nm^{-1} is curve a and that for $\kappa = 1.0$ nm^{-1} is curve b. (A) No calcium, no protamine. Curve c is the structure function for the sugar groups attached to the KDO-core disk in the plane at $z = 0$. In our model, these exhibit Bragg peaks, broadened because of finite-size effects. $S_{OS}(k)$ for $\kappa = 0.3$ nm^{-1} (a) exhibits a small Bragg peak (insert) which has almost vanished for $\kappa = 1.0$ nm^{-1}. This shows that the O-sidechains are more extended in the case of $\kappa = 0.3$ nm^{-1}. (B) With calcium, no protamine. $S_{Ca}(k)$ for $\kappa = 0.3$ nm^{-1} (c) and $\kappa = 1.0$ nm^{-1} (d). (C) With protamine, no calcium. $S_P(k)$ for $\kappa = 0.3$ nm^{-1} (c) and $\kappa = 1.0$ nm^{-1} (d). Note the very broad Bragg peaks. (D) With calcium, with protamine. $S_P(k)$ for $\kappa = 0.3$ nm^{-1} (c) and $\kappa = 1.0$ nm^{-1} (d). $S_{Ca}(k)$ for $\kappa = 0.3$ nm^{-1} (e) and $\kappa = 1.0$ nm^{-1} (f).

We made use of structure functions to analyze our simulation data,

$$S(\vec{k}) = (1/N)\left|\sum_{\vec{r}} g(\vec{r})e^{i\vec{k}\cdot x}\right|^2 \quad (4)$$

where $g(\vec{r})$ is the probability of finding an object at point $\vec{r}$. We used

$$S(k) = \langle S(\vec{k})\rangle_{|\vec{k}|} \quad (5)$$

where $\langle ...\rangle_{|\vec{k}|}$ indicates averaging over all wavevectors $\vec{k}$ of a given magnitude. In three dimensions, this represents what one would observe in a neutron or X-ray powder pattern and corresponds to observations made on bacterial surfaces which are oriented randomly. Here we have restricted $\vec{k}$ to lie in the plane parallel to the membrane.

Figure 4 shows the structure function, $S(k)$, for the four cases considered here (with and without calcium and/or protamine), obtained by averaging over wavevectors, $\vec{k}$, lying parallel to the plane of the membrane. Where Figure 3 showed us the distribution of moieties perpendicular to the membrane plane, Figure 4 identifies structures parallel to it. Here we have plotted log[$S(k)$] versus log[k] for the structure functions for the centers of the sugar spheres of the O-sidechains, $S_{OS}(k)$, the protamine spheres, $S_P(k)$, and the calcium spheres, $S_{Ca}(k)$.

Figure 4A shows the structure function for an O-sidechain brush with no protamine or calcium added for $\kappa = 0.3$ nm^{-1} (a) and for $\kappa = 1.0$ nm^{-1} (b). Also shown is the structure function (c) for the centers of the disks representing the projection of the KDO-core−lipid A structure, embedded in the outer membrane, onto the plane at $z = 0$. It exhibits broadened Bragg peaks because of finite-size effects. The slope of the approximately linear

section of $\log[S(k)]$, for $-1.1 < \log[k] < -0.5$, is -1.82. Its value is determined by the fractal dimension of the distribution of disks and sugar groups projected onto the membrane plane and, in the case of the former, should be -2. The difference arises probably because of the small size of the simulation. $S_{OS}(k)$ (a,b) exhibits a small peak at $\log[k] = -0.356$ (arrow) corresponding to a characteristic distance of 1.43 nm, very close to the main peak of $S(k)$ for the base disks (c). The fact that this peak is more pronounced for the case of $\kappa = 0.3$ nm^{-1} (a) than for $\kappa = 1.0$ nm^{-1} (b) supports the result that the chains are extended perpendicular to the membrane plane more so in the former case than in the latter. This is because the stronger electrostatic interaction causes the (net negatively charged) O-sidechains to repel each other more strongly in the former case.

When calcium is added (Figure 4B), this small peak is reduced because the calcium acts as a bridge to cause aggregation of the O-sidechains. The slope of the approximately linear regime of $\log[S_{OS}(k)]$ is again ca. -1.82.

It should be stressed, however, that the calcium bridging resulting in O-sidechain clustering is not static. Both the calcium ions and the O-sidechains exhibit movement similar to that observed when the calcium was absent. The calcium ions move in and out of a complex distribution of dynamic potential minima resulting in a steady-state average distribution, inside of which motion occurs.

Figure 4C shows the effect of adding only protamine outside the brush and allowing the system to relax to equilibrium [Figure 3B]. It can be seen that $S_P(k)$ exhibits a suggestion of a broad peak at $\log[k] = 0.295$, for both values of κ, which corresponds to a length scale of 0.32 nm. This is the approximate distance between the peptide spheres along the model molecule (Figure 1D). Several very broad peaks also appear for $\log[k] \approx -1.0$, but we have not attempted to identify them.

Figure 4D shows the effect of inserting both calcium and protamine into a region outside the O-sidechain brush and allowing the system to relax. As was seen in Figure 3, the calcium forces the protamine to be trapped further from the membrane plane ($z = 0$). The peak in curves c and d at $\log[k] = 0.295$ is unchanged from that in Figure 4C, showing that calcium does not alter the average conformation of protamine molecules when trapped inside the O-sidechain brush.

Conclusions

We carried out experiments to study the inhibitory effect of protamine upon B-band *P. aeruginosa* PA01 and three *E. coli* strains: Ec1 (EC961019, serotype O157:H7, Health Canada), Ec17 (EC970112, O157:H7, Health Canada), and Ec22 (ATCC 25922, O6) in the presence and absence of Ca^{2+} and Mg^{2+}.

We also modeled the electrostatic interactions between five protamine molecules and the surface of a Gram-negative bacterium possessing charged O-sidechains in the presence/absence of calcium ions in an aqueous solution. We chose the O-sidechain polysaccharide to be that of the B-band lipopolysaccharide of *P. aeruginosa* PA01 which comprises a trisaccharide unit possessing the charge sequence +, −, −. We modeled the protamine Y1 from Atlantic herring. The aqueous solution, containing monovalent ions, was described by linearized Poisson−Boltzmann theory with a Debye screening length κ^{-1}. We considered $\kappa^{-1} = 1.0$ nm and $\kappa^{-1} = 3.33$ nm. The first choice represents the ionic strength in a physiological solution, ∼100 mM, while the second is ∼10 mM. Our findings and conclusions are as follows:

[1] A high concentration of calcium ions equal in number to $^1/_2$ of the net charge on all the O-sidechains brought about a slight polysaccharide chain collapse. The calcium ions formed dynamic bridges, exhibiting a high lateral diffusion, between the net negatively charged O-sidechains.

[2] Without the presence of added calcium, all five protamine molecules became trapped in the charged polysaccharide O-sidechain. The probability of finding segments of protamine molecules closer to the membrane plane than ∼0.5 nm was effectively zero.

[3] If only monovalent ions are present in the aqueous solution initially, then, if either calcium or protamine is separately added, their distributions along the *z*-axis, away from the membrane plane, were essentially independent of the monovalent ion concentrations defined by $\kappa = 0.3$ nm^{-1} and for $\kappa = 1.0$ nm^{-1}. It cannot be concluded from this, however, that the MIC determined in complex growth media will be independent of monovalent salt concentration. Protamine distribution, in the presence of divalent cations, does depend on monovalent ion concentration. Even in the absence of additional Ca^{2+} ions, complex culture media contain an intrinsic variety of multivalent ions (sugars, vitamins, peptides, salts, etc.). Both our simulations and experimental work[5,7] show that MIC should depend on monovalent salt concentration.

[4] When calcium and protamine are present simultaneously, the effects depend strongly upon the monovalent ion concentration. When $\kappa = 1.0$ nm^{-1}, the protamine distribution becomes elongated along the *z*-axis so that the probability of being near the membrane decreases. When $\kappa = 0.3$ nm^{-1}, the entire distribution is shifted toward higher values of *z*.

[5] We predict that the effect of the addition of calcium ions will be to *increase* the MIC compared to when calcium is not added. The MIC will be *higher* for the case of $\kappa = 0.3$ nm^{-1} than for the case of $\kappa = 1.0$ nm^{-1}.

[6] Our experiments confirmed our modeling predictions that the addition of Ca^{2+} significantly reduced the inhibitory effect of protamine. This would also confirm the importance of electrostatic interactions during the first step in protamine's antibacterial mode of action. Interestingly, addition of Mg^{2+} had a significantly smaller effect on the MICs, and we hypothesize that Mg^{2+} was less effective in screening protamine out of the polyelectrolyte brush.

Our predictions concerning protamine distribution might be tested experimentally using neutron or synchrotron sources.

Here we considered only electrostatic interactions and have not considered hydrogen bonding. It is possible that the effects of allowing hydrogen bonding within the O-sidechain brush and between protamine and the O-sidechains could be important. This would imply that protamine molecules bind more tightly than simply electrostatic interactions. Since the hydrogen bonding possibilities are not dependent upon position along the chain, we do not expect our conclusions to be altered by hydrogen bonding.

Acknowledgment. This research was supported by the Natural Sciences and Engineering Research Council (NSERC) of Canada through its support of the MNG project "Structure−Function Relations of Food Biopolymers" and through grants to D.A.P., T.A.G., T.J.B., and M.H.J.

LA030193E